J. Phys.: Condens. Matter **11** (1999) R295–R322. Printed in the UK PII: S0953-8984(99)99455-9

REVIEW ARTICLE

Models of image contrast in scanning force microscopy on insulators

A L Shluger†, A I Livshits†‡, A S Foster† and C R A Catlow‡

† Department of Physics and Astronomy, University College London, Gower Street, London WC1E 6BT, UK
‡ The Royal Institution of Great Britain, 21 Albemarle Street, London W1X 4BS, UK

Received 18 November 1998

Abstract. We review the results of theoretical modelling of scanning force microscopy and discuss the possibility of obtaining atomic and chemical resolution in contact and non-contact mode SFM, and a related issue of a working model for interpretation of SFM images. As a prototype system we consider the interactions of hard tips with softer alkali halide surfaces in UHV. We briefly review experimental data, then discuss results of static atomistic simulations and molecular dynamical modelling of contact SFM to test some of the assumptions of intuitive SFM models. Then we illustrate the shortcomings of contact SFM by considering an image of a point defect. The mechanism of resolution in non-contact SFM and the effect of avalanche tip–surface adhesion are discussed next. We conclude by discussing the status of SFM with atomic resolution.

(Some figures in this article appear in colour in the electronic version; see `www.iop.org`)

1. Introduction

Scanning force microscopy (SFM) is used routinely in many branches of science and technology, spanning from medicine and biology to nano-technology. The range of applications includes surface topography, parameters of film growth, measurements of adhesion, friction, studies of lubrication, dielectric and magnetic properties, contact charging and many other phenomena from the micrometre down to the sub-nanometre scale. Several recent reviews of the technique and its applications can be found in [1]. Tribological aspects of SFM applications are reviewed in [2] and [3]. Specific issues of SFM applications to organic materials are considered in [4], and to nanoscale studies of ferroelectric domains in [5]. Many of the surface properties which could be studied by SFM are directly related to materials chemistry, for example, surface topography and chemical structure, reactivity of specific surface areas and sites, adsorption of molecules and clusters, parameters of atomic and molecular diffusion, chemical reactions and reaction products. However, studies of these properties at the sub-nanometre end of the scale still remain one of the main challenges of the technique. Recent rapid developments in SFM instrumentation (see, for example, [6–13]) offer exciting new possibilities for materials physics and chemistry, and other applications. However, the maturity of the technique is also characterized by the level of its theoretical understanding and quality of the models used for interpretation of the results. We will critically review some of these models used in SFM studies on insulators and will demonstrate what atomistic modelling and simulation can contribute to their further rectification and development.

0953-8984/99/260295+28$19.50

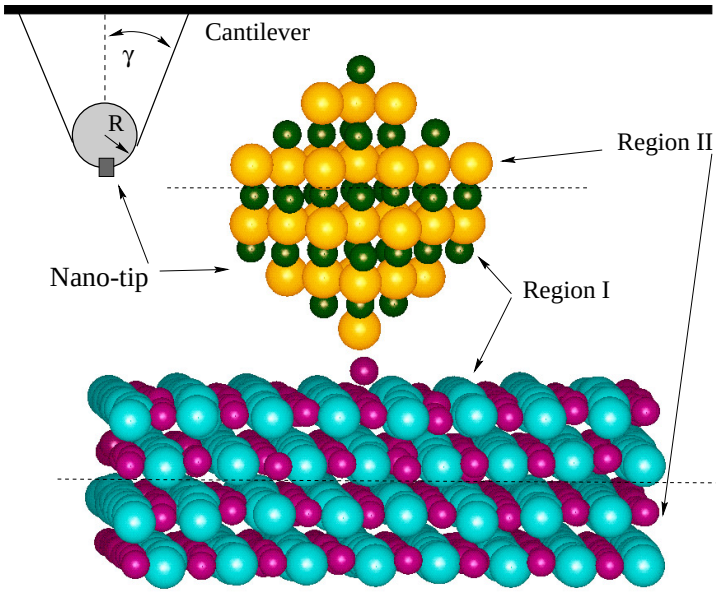

Figure 1. A schematic of the SFM tip and a snapshot of a representative atomic configuration of the MgO nano-tip interacting with the LiF surface. The tip is modelled by a cone with angle γ and a sphere of radius R at the end. The nano-tip is embedded at the bottom of the sphere. Note the strong displacement of the Li ion from the surface towards the tip.

Information about surface properties is obtained in SFM by monitoring the interaction between a tip attached to a cantilever and the surface under study (see figure 1). The cantilever can be described as having effective spring constants corresponding to different degrees of freedom—normal, lateral and torsional (which are not entirely independent), and an SFM signal is detected by measuring cantilever deflections. For instance, to study adhesion between tip and surface, one can measure the dependence of the force on the distance between the SFM tip and surface at fixed lateral tip positions, which is called force spectroscopy [14, 15]. To study surface topography or friction, one monitors normal or lateral cantilever deflections as the tip scans the surface continuously along some trajectory. This information is processed [16] and presented in the form of three-dimensional topographic maps which are interpreted as a surface image. If the dimensions and shape of the tip are comparable to those of the surface topography, the image is a convolution of the two: surface topography and tip shape. These and other artifacts in SFM topographic imaging on microscopic scale are discussed, for example, in [17]. However, in this review we are predominantly concerned with understanding of contrast in SFM images on the nanoscale. In some cases topographic representations of the tip–surface interaction obtained on this scale look like periodic arrangements of individual atom sized features separated by distances comparable to the interatomic separation at the surface known from other data. It is indeed extremely tempting to interpret these image features as surface atoms or molecules. Although the term ‘atomic resolution’ is often used in describing these images, its meaning is not well defined. It is now widely accepted that atomic resolution is achieved if it is possible to distinguish a surface defect which has atomic dimensions, such as a step edge or an impurity atom, from a periodic arrangement of image features. However, as we will see below, even in this case the largest cantilever deflections from the set-point do not necessarily correspond to the average positions of the surface atoms or molecules.

Before discussing how atom size features in the topographic image result from the interaction of two macroscopic bodies—tip and sample, we need, however, to specify further the main forces involved and the conditions of imaging.

Some of the long-range forces [15, 18] between tips and surfaces include the van der Waals attraction [19–23], a capillary force due to the presence of fluid films at the surface when imaging in liquid or air (see, for example, [24, 25]), and electrostatic forces, including those due to tip and surface polarization (image forces), and due to patch charges and the surface charging after cleavage [15]. In intimate contact, the repulsive and attractive short-range forces between a smaller number of tip and sample atoms in the contact area (see figure 1) play a decisive role in regulating the force equilibrium. In order to have a convenient terminology, we will refer to these latter forces as comprising the chemical interaction force between the tip and sample.

The van der Waals is the most universal and in many cases the strongest tip–surface interaction which greatly influenced the development of the SFM technique. Since the tip–surface interaction is measured via cantilever deflections, the SFM sensitivity could be enhanced by making the normal cantilever spring-constant, k, smaller. However, this has a negative effect: when the van der Waals force starts to increase faster than k, the cantilever experiences mechanical instability. Therefore with soft cantilevers the tip cannot approach the surface smoothly but jumps into hard contact at some critical distance. It can then be operated only in hard contact (hence 'contact mode' SFM) which in many cases proves to be too invasive. One way to provide a softer tip–surface contact is to immerse the whole set-up in liquid with dielectric properties which effectively screen the van der Waals interaction between tip and surface and prevent jump-to-contact [26–28]. Although this approach proved to be very fruitful in studies of biological systems, crystal growth and dissolution, and in other applications, it is obviously not universal. Another technique, which is becoming increasingly popular, is to oscillate the cantilever with large amplitude and to monitor the changes in parameters of these oscillations induced by the tip–surface interaction [7]. Due to the large oscillation amplitude, the cantilever elastic force always exceeds the van der Waals force even at very small tip–surface separations, preventing the tip from jumping into contact [29]. Application of frequency modulation and efficient electronics allows one to measure very small changes in the cantilever oscillation frequency. Therefore the shortest probing distance between tip apex and surface can be larger than the characteristic equilibrium bondlengths in the system (i.e. than hard contact distance). Hence this technique is called non-contact (NC) mode. Note that 'contact' in this context is defined only on an intuitive level and is very difficult to specify more clearly experimentally.

The macroscopic van der Waals force is not site-specific and therefore contrast in SFM images is defined by the interplay between van der Waals and chemical forces. The latter strongly depend on the geometric and chemical structure of a specific tip and surface. Therefore interpretation of SFM images in terms of chemical identity of the surface atoms, and understanding of most of the contact phenomena, even for relatively simple systems, still relies on intuition rather than on established models. Unlike STM where the Tersoff–Hamann model [30] is widely used as the basis for interpretation of experimental images, there is not such a basic model in contact SFM. An early example of such a model has been that of one atom tip apex and rigid surface. A 'contact hard sphere' approximation was used for interpretation of SFM images obtained in air and in ultrahigh vacuum (UHV) in which a rigid surface composed of hard spheres with ionic radii was profiled by another hard sphere representing the tip apex atom [31–34]. However, it was soon recognized that the tip and surface deformation, and even wear during scanning in contact can be very significant [35]. Furthermore, many surfaces in air adsorb water and other gases and it has been shown that their images and tribological

properties strongly depend on humidity (see, for example, [36, 37]). The question which still remains unresolved is whether water present at these surfaces serves just as an inert lubricant which does not participate in the image formation. Interpretation of the tip–surface interaction and images obtained in liquids is even more complex due to contribution of liquid molecules to the force on the tip [38, 39].

A large number of technological and fundamental scientific problems lead one to perform SFM measurements on clean surfaces in vacuum. Contact SFM in UHV has also been used for basic surface studies and for developing and testing models for image interpretation. The surfaces of simple cubic alkali halides played an archetypal role in these studies [35, 40] which is in many respects similar to that of the Si and HOPG surfaces in STM studies. The alkali halides were also among the first to be studied [41, 42] by non-contact mode SFM, but the theoretical understanding of the mechanisms of both contact and non-contact SFM is still developing.

In this review we test some of the assumptions of intuitive SFM models, present the results of extensive theoretical modelling of the SFM imaging of ionic surfaces and discuss the possibility to obtain atomic and chemical resolution in contact and non-contact mode SFM and a related issue of a working model for interpretation of SFM images in UHV. First, we briefly review the experimental SFM images on insulators and discuss theoretical models of contact SFM. We illustrate the shortcomings of this technique by considering imaging of a point defect. Then we turn to the question of resolution in non-contact SFM, and discuss how it may be affected by avalanche adhesion. Finally, the status of SFM with atomic resolution is discussed.

2. SFM imaging of insulators

Surfaces of many insulators have been studied using contact SFM over the last ten years. Atomic or molecular periodicity has been observed in SFM images of almost all alkali halides [31, 36, 43], several alkaline-earth fluorides [36, 44], silver bromide [45, 46], polished sapphire [47], magnesium oxide [33, 34], strontium titanate $SrTiO_3$ [48], anhydrite ($CaSO_4$) [49, 50], V_2O_5 and V_6O_{13} [51] and the natural zeolites, stilbite and heulandite [52], all obtained in air. However, the interpretation of these images is still unclear because of many uncontrollable factors which can affect the image. The most important of those include the tip structure and the role of ambient conditions, in particular water adsorbed both on the tip and surface. To eliminate the latter factor some experiments were carried out in UHV [53–55]. In unparalleled low temperature UHV SFM experiments [35] on KBr, Giessibl and Binnig have brought contact SFM to the limit of sensitivity and have demonstrated that one can obtain periodic images without visible surface wear up to the loads of about 3 nN. Although step edges on surfaces were resolved [55] and occasional observations of point defects were reported [54, 56], still the origins of the image contrast remained unclear. Observations of periodic images up to large tip loads, where wear could be expected, and friction studies suggested that the image periodicity may reflect the periodic character of the tip surface interaction rather than the average positions of the surface atoms or molecules, and 'point defects' could be just image artifacts. It has been realized that in most cases the tip does not interact individually with surface atoms and a periodic image can result from extremely complex tip–surface interaction. Observation of surface point defects became the most convincing test of SFM resolution. However, many attempts to systematically observe and identify point defects, such as specially introduced impurities, in contact mode proved unsuccessful.

Several point-defect-like features were observed recently over a long time period using NC-SFM on semiconductor [9, 57–59] and alkali halide [41, 60] surfaces. It is generally

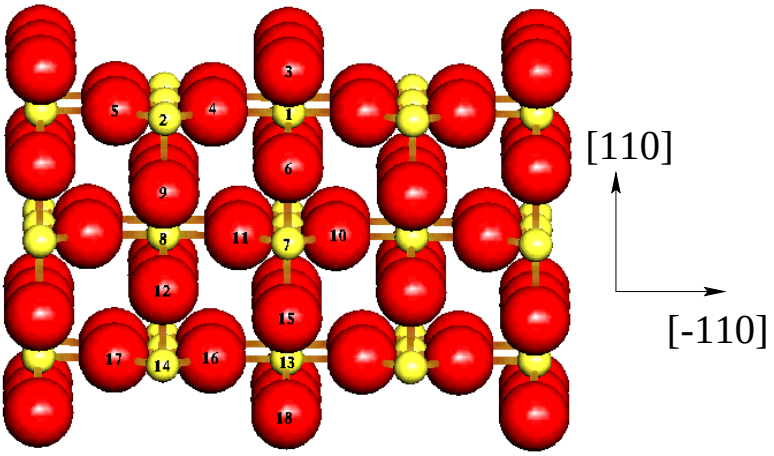

Figure 2. The geometric structure of the (110) TiO_2 surface.

accepted that the tip–surface interaction in NC-SFM is much less invasive than in contact mode. The stability of images suggests that these could be genuine defects. Nevertheless it was not possible to prove either the nature of the defect nor even to determine the surface sublattice (cation or anion) in which they are present. This raises a conceptual question: suppose 'atomic resolution' is achieved; how can we prove the chemical nature of resolved regular image features and defects? It is easier to understand this crucial feature by taking an example, for which we have chosen TiO_2.

Due to its many applications and their dependence on surface properties, TiO_2 is easily one of the most widely studied oxide surfaces in surface science. This popularity also makes it a very attractive candidate for comparing different and developing new experimental techniques. A comprehensive review of these techniques was undertaken by Henrich [61] in 1985, where the stoichiometric (110) 1×1 (0.649×0.296 nm^2) surface was established as the most stable. This surface was more recently studied by surface x-ray diffraction [62] medium-energy back-scattering electron diffraction [63], STM [64–66], non-contact SFM [57] and a combination of both techniques [59]. These experimental results are well supported by theoretical calculations of the surface structure and properties using various techniques [67–69]. The experimental results and theoretical modelling agree in that the 1×1 surface is composed of alternating rows of exposed fivefold coordinated Ti ions and the bridging O ridges, which are displaced further out from the surface plane (see figure 2). Since the Ti and O rows are equivalently spaced, the question arises how to distinguish between them in STM and SFM images.

The relatively narrow bandgap of TiO_2 allows one to make both STM and SFM experiments. Each of the probe microscopy studies came to the conclusion that they imaged the familiar 1×1 surface unit cell, although via different sub-lattices. The interpretation of STM experiments using the Tersoff–Hamann theory [30] suggests [68, 70] that STM images the fivefold coordinated Ti ions. To interpret NC-SFM images, Iwasawa [59] simply makes the assumption that the imaged contrast is due to the surface topography, and that the protruding bridging oxygen rows (see figure 2) are being imaged. Since the 'bright spots' in the NC-SFM image are due to the strongest tip–surface attraction, the validity of this interpretation depends entirely on the unknown tip structure. For instance, oxide at the end of the tip will interact with the TiO_2 surface differently than silicon or metal. A more clear-cut answer could come from imaging of ions adsorbed on the surface. Iwasawa [59] adsorbed formate anions onto the TiO_2 surface and then imaged them using STM. The adsorbed formate ions can interact

primarily with the accessible Ti cations, and the STM images show clearly bright spots on the resolved titanium rows, as expected. However, the NC-SFM images of individual formate ions on the same surface [58] are much less clear. Their interpretation, based on the mechanistic model that NC-SFM images physical topography of the surface, suggests that formate ions are bridging two Ti rows. Although the model of the formate ion adsorption looks plausible it cannot be justified directly from the image contrast and requires further analysis based on clearer understanding of the tip–surface interaction.

These results present an example of experimental approach to resolving the surface structure combining different methods and using molecular adsorption to 'mark' one type of surface ions. They provide a lot of 'food' for theoretical simulations, but leave the main issue of chemical resolution largely unresolved. It is unclear whether the NC-SFM image interpretation based on the model that what sticks out should interact more strongly with the tip is correct, and whether NC-SFM can leave adsorbed molecule unperturbed. These are general issues which should be addressed by theory.

3. Theoretical models of SFM images

Immediate interpretations of experimental periodic images are based either on the apparent resemblance of the image with some expected surface atomic structure, or on the 'contact hard sphere' approximation mentioned above in which a rigid surface composed of hard spheres with ionic radii is profiled by another hard sphere representing the tip asperity [31–33]. In [36], periodic images were obtained experimentally for nine alkali halides using a Nanoscope II in air at controlled humidity and using the same tip. To check the 'contact hard sphere' approximation, the principal Fourier component giving the lattice period was divided by the integrated Fourier background to define a figure of merit of the atomic periodicity of the SFM images. This was plotted against R_+/R_-, the ratio of cation and anion radii. If the ions are really being imaged as hard repulsive spheres, the image contrast should peak for large or small R_+/R_-, and vanish when $R_+/R_- = 1$. However, no discernible correlation with R_+/R_- was found. A more sophisticated method of image interpretation used in [51] and [71] is based on comparison of observed images with surface total electron density plots. The basis for this comparison is unclear. As we will see below there are reasons to believe that both this and the one atom tip and rigid surface models are too simplistic to provide reliable understanding and interpretation of contact SFM images.

Theoretical modelling based on an atomistic approach, developed over the years, demonstrated the main forces involved in contrast formation and the importance of the tip and surface deformation during scanning. Van Labeke *et al* [72] and then Giessibl proposed [35, 73] that, for an atomically sharp tip and a rigid ionic surface, the main interactions responsible for the image contrast are between the surface electrostatic potential and the dipoles induced by this exponentially decaying potential on the foremost tip ions. *Ab initio* calculations [74] have demonstrated that sharp ionic tips, such as oxides, produce a slowly decaying electrostatic potential which polarizes the surface which also makes a significant contribution to the image contrast. The importance of electronic structure was highlighted in [75], and the effects which the tip atomic profile may have on observed images were considered in [76]. Several models of the tip interaction with ionic surfaces, accounting for distortions of both the tip and surface, have been analysed using static atomistic simulation and quantum-chemical techniques [36, 77–79]. In particular, the images of the NaCl surface by a diamond tip have been calculated by Tang *et al* [77, 79]. These studies have demonstrated that the tip and the surface can be considered as separate weakly interacting systems only at large ($>$3–4 Å) distances. At shorter distances, the chemical interaction between the tip and surface and the surface deformation are very

strong. An even more complex picture of the tip–surface interaction was revealed by extensive molecular dynamics calculations [80, 81].

Modelling of NC-SFM has also made rapid progress over the last two years [29, 82, 83, 90]. It includes two main components: (i) modelling of cantilever oscillations using known tip–surface forces; (ii) calculation of the tip–surface forces. The first problem has been considered in detail in conjunction with the tapping mode of SFM operation [82, 84–86] and recently also with respect to NC-SFM [29, 82, 83, 87–90]. The tip–surface forces have been reviewed in several publications [15, 29, 91, 92]. However, the chemical component of the tip–surface interaction which is responsible for adhesion and in most cases for the contrast formation is difficult to quantify without atomistic modelling of particular systems. The interaction of model Si tips with the Si(111) 7×7 surface were calculated in [93], and images of several ionic crystals were calculated in [94].

In spite of significant progress both in understanding of interactions involved in SFM contrast formation and in modelling adhesion, indentation and surface scanning the question remains: can the relatively simple or more sophisticated models provide unique interpretation of SFM images and help to identify, study and modify surface defects, active sites or adsorbed molecules by the tip? Can atomistic simulation of the tip–surface interaction be used routinely for image interpretation? To answer these questions, the accuracy of existing SFM models should be analysed in more detail.

4. Computer modelling of SFM imaging

4.1. Tip models

The most important component of any SFM is indeed the tip. Studying specially prepared regular surface features comparable to the size of the tip, i.e. from 10 nm to several μm, one can reconstruct the mesoscopic shape of the tip relevant to the imaging with reasonable accuracy [95–99]. Note that any surface feature which is sharper than the probing tip is effectively imaging the tip. One can also recover some information about the tip shape from images of strongly corrugated samples [100] and using more direct methods such as STEM [101]. Therefore the macroscopic shape and dimensions of many new commercial and specially fabricated tips are known. They can change significantly, though, due to cleaning by ion sputtering or interaction with the surface during scanning [101].

Information about tip shape, dimensions and chemical composition is necessary to calculate the van der Waals interaction with the sample. The expressions have been derived for the van der Waals interaction between macroscopic tips of different shape and plane surfaces as a function of Hamaker constant, geometric parameters of the tip and the distance between the end of the tip and the surface plane [29, 102]. However, the latter is not well defined on the atomic scale. To avoid significant errors at short distances and at hard tip–surface contact one should consider the van der Waals interaction between the tip and surface atoms in the contact area atomistically. Therefore in many calculations the tip and the semi-infinite sample are divided into two regions (see figure 1): (i) the parts of the tip and the sample far from the contact area are considered as rigid macroscopic bodies which interact only via the van der Waals and the electrostatic interactions; (ii) the very end of the tip apex and several surface layers shown in figure 1 are treated atomistically. The rigid macroscopic part of the tip in most calculations has conical or pyramidal form with a spherical apex of radius R (see, for example, [80, 103, 104]).

However, the image contrast is determined by the chemical interaction of the tip apex with the surface. Calculation of this interaction requires detailed knowledge of its atomistic

structure. Commercially available tips used in most experiments are microfabricated from silicon or silicon nitride. In some cases home-made metallic [105], diamond [106] and specially coated or modified tips are employed [101]. Recent experiments have demonstrated that metal coated tips are not reliable enough to yield repeatable data, and that silicon tips are more reliable for this purpose [101]. Although metallic tips can be better characterized by field ion microscopy [107], they are not used routinely in SFM studies. Most of the silicon, silicon nitride or metallic tips are covered by a native oxide layer which is thought to be removed in some experiments by sputtering with the Ar^+ ions. However, the atomistic structure and geometry of the very end of the tip is practically impossible to control, except for metallic tips.

A possible model of the Si tip shape and atomistic structure based on SEM data and qualitative considerations was proposed in [108]. Some of the factors which determine the Si tip structure could be summarized as follows: the silicon nano-tip should bear the characteristic features of the most stable Si(111) (7×7) surface; it may have some residual oxide layer or oxygen adsorbed on it; it can be contaminated by hydrogen or water residual in the vacuum chamber; it can also be contaminated by the surface material. The charge state of adsorbed species, which affects the extent of the tip modification, depends on the tip and surface electronic structure.

Due to uncertainty in the tip apex structure, simplified models of aluminium [76], diamond [77, 79, 109, 110], silicon [93], SiO_2 [36, 111] and MgO [78, 112] tips are used in most computational studies. Another issue which affects a particular choice of the tip model is that the interaction in heterogeneous interface systems (for instance, Si tip and NaCl surface) is not easy to describe. Although a thorough justification of the tip model may not be necessary in modelling concerned with general qualitative effects, interpretation of particular experimental images requires more detailed knowledge. Therefore a comparative study of several Si tip structures has recently been performed in [113] using a periodic density functional theory method. Since all atomistic tip models are inevitably finite clusters, the aim of [113] was to study how well a finite cluster may represent the macroscopic tip surface, and how the electrostatic tip potential depends on its contamination by different species.

An Si_{33} cluster [114] (see figure 3) was used as a basic silicon tip model in [113]. This model possesses the structural features characteristic of the DAS Si(111) (7×7) reconstruction model [115]: the dimer pairs and adatoms. To check whether this really is a representative model for the Si(111) surface, the geometric and electronic structure, and the electrostatic potential for the (5×5) surface reconstruction (see figure 3) were calculated. The latter is the smallest model containing the same basic structural features as the (7×7) reconstruction [93]. The electron density distributions and the electrostatic potentials near similar features on the Si surface and the Si_{33} cluster proved to be very similar. In particular, a charge density integration around the surface and cluster adatoms gave an almost identical charge distribution. The three-coordinated adatom possesses a dangling bond and is the most chemically active surface site [116]. Two other tip models were also considered: (i) Assuming that the adatoms, which are also the most outstanding surface atoms, are most likely to serve as the probe species, they can be modelled by a smaller cluster. The calculations of electrostatic potentials show that a surface adatom can be well represented by a smaller Si_{10} cluster (see figure 3). This cluster was compared with the hydrogen terminated Si_{10} cluster used by Pérez *et al* [93] to model tip–surface interactions. Our calculations show that hydrogen termination of the base of the Si_{10} cluster has negligible effects on the electrostatic potential and the charge density near the adatom. (ii) To model a more inert tip, an Si_{29} cluster can be used, which does not have the four adatoms of the Si_{33} cluster.

The most important component of the tip–surface interaction with ionic surfaces at long distances in NC-SFM is the electrostatics [94]. Therefore the gradient of the electrostatic

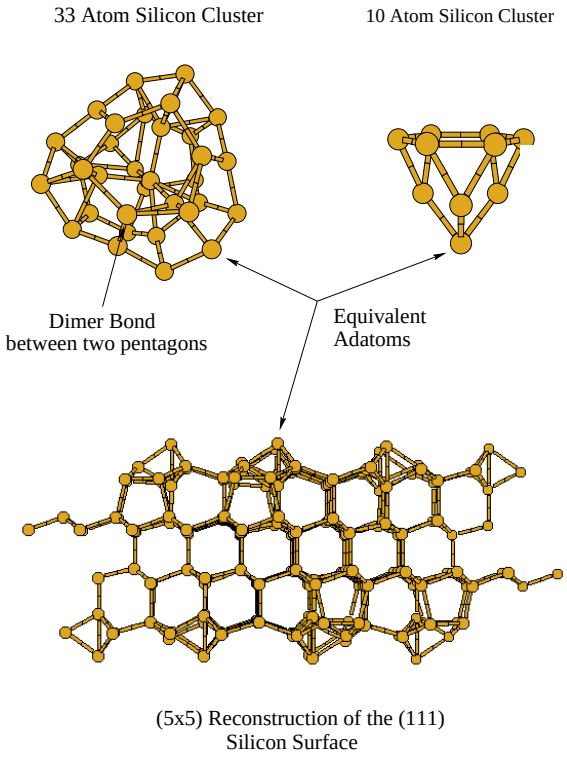

Figure 3. The geometric structures of the Si(111) (5×5) reconstructed surface, and of the Si_{33} and Si_{10} clusters used to simulate the SFM tips.

potential is the most meaningful criterion for comparison of different tips. In this discussion we assume that low-coordinated tip sites are most likely to serve as surface probes. The electrostatic potentials near the adatom on the Si(111) surface and that produced by an Si_{10} cluster are shown in figures 4(a) and (b). As one can see, despite the surface polarization by the low-coordinated atoms, the electrostatic potential in both cases decays very quickly. Silicon tips contaminated by several species which can be present in UHV chamber were also considered. In particular, water is known to dissociate to the hydrogen atom and the OH radical on the Si surface [117]. Therefore the silicon tip with these species adsorbed on the adatom site, which is known to be the most reactive surface site [116], was considered. To model the residual oxide and the silicon tip contamination by oxygen due to contact with an oxide surface, an oxygen atom was adsorbed on the tip adatom. Test calculations for the Si_{33} and Si_{10} clusters with adsorbed species gave very similar results. Therefore in figures 4(c)–(e) we present the electrostatic potentials calculated only for the Si_{10} cluster.

One can see that the adsorption of the hydrogen atom does not significantly affect the tip potential. However, the adsorption of a polar OH group produces a much more longer range potential which extends to about 2 Å from the terminating H atom (figure 4(d)). An even stronger electrostatic potential is produced by the tip with the oxygen atom adsorbed on the adatom site (see figure 4(e)), which is caused by the negative oxygen charge due to electron density flow from the nearest silicon atoms to the oxygen. Comparison with the calculation of the electrostatic potential produced by the oxygen corner of $(MgO)_{32}$ cluster modelling the

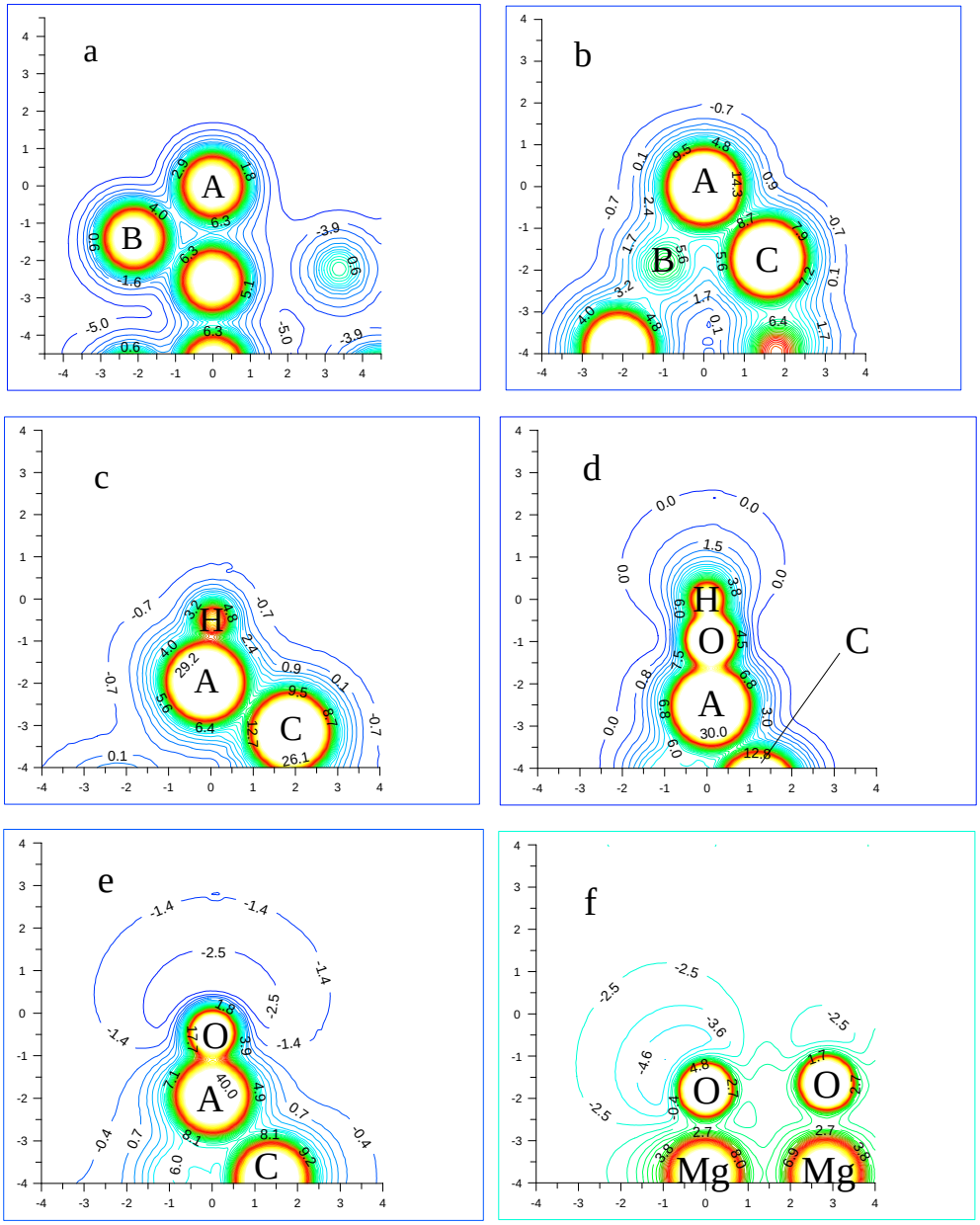

Figure 4. Sections of the electrostatic potential calculated for several silicon structures and the $(MgO)_{32}$ cube using a periodic DFT method. The scale on the axes is in ångstroms and the units of the contours are eV. A, B and C represent equivalent atoms in the Si surface and Si_{10} cluster; atom A is the adatom. (a) The adatom site on the reconstructed Si(111) (5×5) surface; (b) the adatom modelled by the Si_{10} cluster; (c) the hydrogen atom adsorbed on the Si adatom in the Si_{10} cluster; (d) the OH radical adsorbed on the Si adatom in the Si_{10} cluster; (e) the oxygen atom adsorbed on the Si adatom in the Si_{10} cluster; (f) the oxygen corner of the $(MgO)_{32}$ cube; the potential is shown in the plane which includes the $\langle 111 \rangle$ cube axis through the oxygen tip ion. Note that in (b) the section is made in the symmetry plane, whereas in (c)–(e) the section is through atoms A and C, and the adsorbed species.

MgO tip (figure 4(f)) shows that the gradients of the electrostatic potential produced by this tip and the Si tip with the adsorbed oxygen atom are very similar.

These calculations demonstrate that at relatively large tip–surface distances characteristic, for example, of NC-SFM, simplified tip models which can reproduce correctly the ionic electrostatic interaction with the surface can be representative of a wide class of tip materials. Tip contamination strongly changes its chemical properties, determined in the previous example by silicon dangling bonds. In hard contact, the tip is much more likely to be contaminated by the surface material during scanning and therefore its chemical structure and elastic properties are even more important. The diamond [77, 79] and MgO [78, 80, 81, 112] cluster models were used to simulate the contact SFM imaging of alkali halides. The plausibility of these models can be only judged by comparing their predictions with experimental data.

In the following sections we will review the results of computer modelling of contact and non-contact SFM to test the limits of the simple SFM models, and to discuss why it may be so difficult to observe point impurities at surfaces with SFM. But before that a short discussion of computational techniques used in SFM simulations is required.

4.2. Computational techniques

SFM simulations involve calculations of the force exerted on the tip as a function of the tip position with respect to the sample surface. Studies of the tip and surface adhesion, surface indentation by the tip, or contact phenomena can be carried out at some selected surface points as a function of vertical tip displacements. Construction of the surface image in contact or non-contact mode requires much more extensive calculations of three-dimensional force-fields. These calculations are made using fairly standard static and molecular dynamics techniques which are described in original publications. Therefore we confine our discussion to peculiar issues of SFM modelling.

(i) Calculations of metal–insulator interfaces require a careful account of the image forces. The situation is further complicated by the fact that most of the doped silicon and metal tips used in experiments are covered by an oxide layer, the thickness and structure of which is difficult to control. It is therefore not surprising that tips made of insulating materials (diamond, SiO_2 and MgO) are used in most SFM simulations on ionic surfaces, and metallic tips on metal surfaces, respectively. Although there are many cases where these are good models, the role of image forces certainly requires detailed study.

(ii) Although studies of some contact phenomena [75, 118] and even extensive calculations for constant height scanlines [93] can be done using high-quality quantum mechanical methods, these methods are still too expensive for routine image modelling. Therefore classical atomistic simulation and molecular dynamics techniques are used much more often. However, here one encounters the problem of validation of the interatomic potentials. For ionic systems, such as MgO tip and LiF surface, this is more a question of consistency of different sets of parameters [78]. However, the parameters of interatomic interactions for 'heterogeneous' systems, such as a diamond tip and the NaCl surface, are much more difficult to justify, especially if one wants to model the dangling carbon bond at the end of the diamond tip [79].

One of the main advantages of using classical techniques is that they allow one to include full tip and lattice relaxation when modelling contact formation and surface scanning. Large displacements of ions inside and out from ionic surfaces or their removal due to adhesion on the tip can be accompanied by strong electron density flow and change the charge states of ions. This can invalidate the use of interatomic potentials in atomistic

simulations. For the alkali halide and MgO surfaces this issue has been addressed in [80] and [118], where the electronic structure of these systems for characteristic displacements of the surface ions was calculated using different quantum mechanical methods. The results of these calculations supported the applicability of an ionic model and corresponding set of potentials for the interaction of ionic tips with ionic surfaces. In this case even strong displacements of ions and their adsorption onto the tip is not accompanied by significant charge redistribution, which is not the case, though, for the interaction of, for example, the Si tip with the surfaces of NaCl and MgO. The calculations [113] demonstrated that chemisorption of the surface anion onto the tip can be accompanied by a dramatic electron density redistribution within the tip and surface.

(iii) Another issue concerns the simulation technique. Static methods based on the total energy minimization are well suited for modelling very slow adiabatic processes at low temperature. In this case the force on the tip is calculated by differentiating the potential energy of the system with respect to the tip normal or lateral displacements [119]. However, as the tip moves with respect to the surface, the potential energy for the surface and tip ions changes constantly. Barriers between some potential wells can diminish and thermally activated jumps [120], and even tunnelling of atoms [121] between different positions within the surface or between the tip and the surface, can become important. The thermally activated atomic jumps can be accounted for more effectively in molecular dynamics calculations, but then the relative speed of the tip motion with respect to the surface becomes an important parameter. The slowest scanning velocities practical for the fastest workstations are about 1 m s^{-1}. This is several orders of magnitude faster than experimental velocities. However, what matters is that the tip displacement of 1 Å takes 100 picoseconds which allows most of the relaxation processes within the tip and the sample to proceed adiabatically with respect to the tip motion. Nevertheless, the calculations [80] demonstrate that these are about the fastest possible velocities for SFM simulations: if the tip moves faster the results depend on the tip velocity. Finally we should note that since the surface scanning, especially in contact, can be accompanied by strong ionic displacements and adsorption/desorption of ions on the tip, continuous tip motion and careful account of the energy dissipation are needed for meaningful analysis of molecular dynamics.

4.3. Modelling of contact SFM imaging of perfect surfaces

The key assumptions which would greatly simplify the SFM model are those of a rigid surface and of a single atom attached to a macroscopic tip. In this model, one can account for all important interactions while still keeping it fairly transparent [72]. Intuitively, it seems appealing to suggest that if one could scan the surface keeping the tip sensibly far, this model could work. Experimentally, in contact SFM, this has so far been achieved only in a very specific UHV-SFM set-up and at low temperature [35]. In most experiments, though, the tip jumps into contact with the surface. Then it may be retracted back from the surface close to the so called 'jump-off point', or pressed against the surface, as scanning begins. The 'jump-off point' determines stability of SFM operation in the attractive regime and corresponds to the tip position on its retraction from the surface where the cantilever bending force exceeds the adhesion force. It depends obviously on the strength of adhesion between tip and surface and is strongly affected by the depth of tip indentation inside the surface (or extent of tip deformation for soft tips) after jump-to-contact which may lead to contamination of the tip by the surface material. The tip surface adhesion and 'jump-off point' change afterwards during scanning if the tip is modified again. Therefore an experimenter is not free to choose the

tip–surface distance; moreover this distance is essentially unknown and cannot be determined experimentally.

Theoretical modelling allows one to obtain a good estimate of the distance range where the surface scanning takes place for given tip and surface. To find where the tip will stop after jump to contact one can calculate the force–distance curves for different macroscopic (the van der Waals interaction) and microscopic (sharpness of the end) tip parameters, as discussed in [80], [81] and [112]. These calculations demonstrate that after jump-to-contact occurs the gap between the MgO tip and the alkali halide surfaces never exceeds 1.5 Å, and when the van der Waals tip–surface interaction is large the tip end penetrates the surface plane. Contact is always accompanied by the strong surface deformation. Therefore all distances in further discussion are given between the unperturbed apex tip atom and the perfect surface plane before contact. The calculations [80, 112] demonstrated that after an indentation of an oxide tip into softer alkali halide surfaces and subsequent retraction the tip is likely to be contaminated by the surface ions. The jump-off distance in most cases does not exceed 2.3 Å.

Shluger *et al* [112] and Tang *et al* [77, 79] performed modelling of SFM scanning of the surfaces of NaCl and other ionic crystals for different tips and scanning conditions using static atomistic simulation techniques. A similar technique was used by Tsujimichi *et al* [111] to simulate SFM images of cleaved mica surfaces; however, the latter calculations did not include the tip and surface relaxation. In the calculations [112] both neutral MgO tips and those modified by dissociated water were used to calculate the constant force scanlines. Surfaces of many oxides are known to be charged because of water dissociation and contain adsorbed protons, hydroxyl groups and their aggregates [122]. This was taken into account in [112] by including a hydroxyl group in the model of the nanoasperity. In this model, a proton adsorbed on the oxygen ion at the cubes' corner oriented towards the sample formed an OH^- group substituting O^{2-}, whereas an OH^- ion was adsorbed on the opposite Mg corner to maintain the tip neutrality. Therefore these corners were locally charged and had different chemical properties with respect to neutral tips. Tang *et al* [77, 79] used a sharp diamond tip and calculated the surface image, moving the tip at different constant heights above the surface. Despite many differences in details, both modellings have demonstrated that even in the 'softest' conditions and in the absence of tip contamination, scanning is likely to involve strong tip and surface deformations. The results suggest that the reversibility of this deformation is a very important condition for periodicity of the tip–surface interaction. In the case of ionic crystals and a not very invasive tip–surface interaction, it can be effectively provided by the strong Coulomb interaction between displaced ions and their vacancies. However, both charged and neutral atomically sharp tips are shown to probe several adjacent ionic rows of the sample. The calculations [112] demonstrated that the correspondence between the scanline extremes (or in other words 'bright' and 'dark' spots in experimental images) and the average positions of the surface ions is more an exception than a rule, and is determined by the details of atomic tip structure. Although such correspondence was demonstrated for a hard and symmetric diamond tip [79], it will not necessarily hold for less symmetric tip orientations. Moreover, the image contrast inverts with the change of polarity of the ion at the end of the tip [112].

If the contact formation or scanning results in the tip being contaminated by a cluster of the surface material, the situation is even more complicated. As demonstrated by molecular dynamics simulations [80, 81], at the initial stages of the surface scanning the structure of the adsorbed cluster changes dramatically which leads to very irregular forces on the tip. However, at small loads tip contamination can also promote periodic SFM imaging if the adsorbed surface material can make stable structures on the tip (see figure 5). This point can be illustrated by the system energy as a function of scanning coordinate for the tip motion along the ⟨110⟩

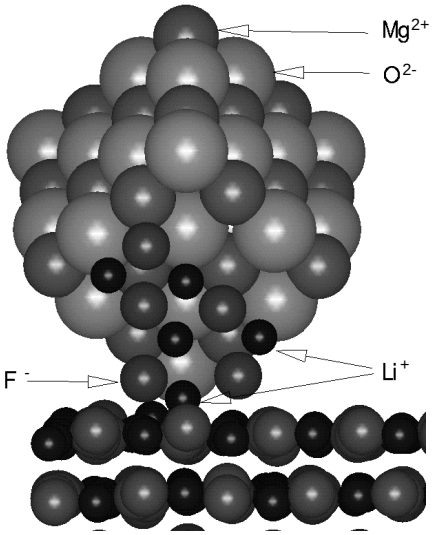

Figure 5. The atomic configurations after formation of the stable structure of the surface material at the end of the MgO tip during scanning of the (100) LiF surface along the ⟨110⟩ axis at the constant height of 2.3 Å.

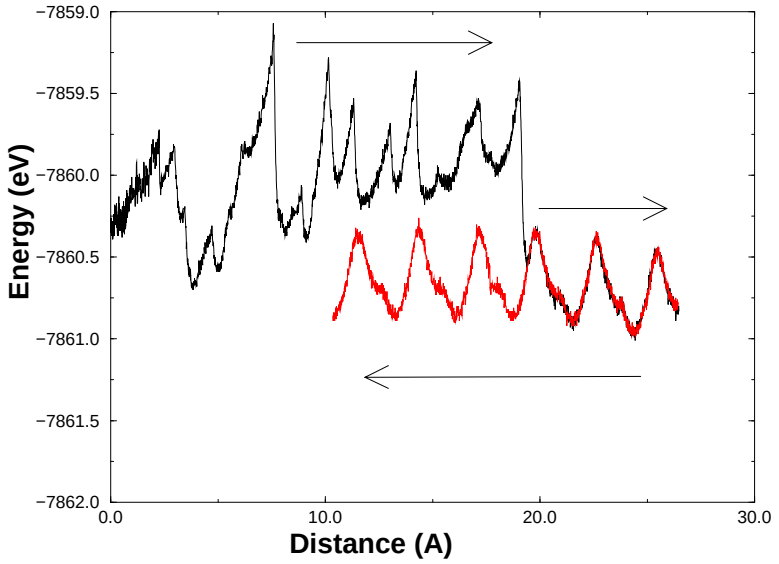

Figure 6. The system total energy against tip position for constant speed tip motion at the constant height 2.3 Å along the ⟨110⟩ surface axis above the (100) LiF surface calculated using the molecular dynamics technique.

direction at the constant height of 2.3 Å shown in figure 6. The initial part of the curve, which is about 18 Å long, demonstrates irregular stick–slip behaviour. It is due to a stick and slip motion of the O^{2-} ion at the end of the MgO tip, which can be explained by the changes of the tip–surface interaction due to the transient adsorption and desorption of Li^{+} and F^{-} ions which effectively charge the tip. Three LiF molecules are adsorbed on the grain of the tip from the

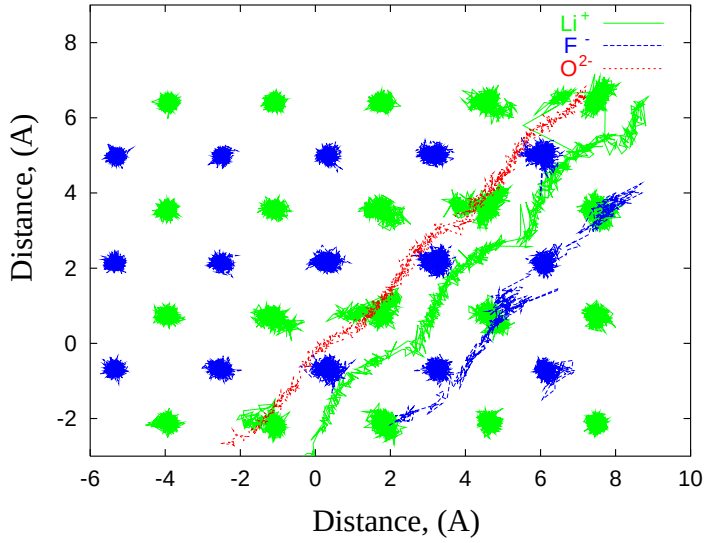

Figure 7. The top view on the trajectories of the surface ions and of the Li^+ and F^- ions adsorbed on the tip, and the O^{2-} ion at the end of the tip, during scanning along the ⟨100⟩ surface axis.

very beginning and do not change their configuration during scanning. Four or five other ions try to accommodate themselves at the tip's end. After one or several dramatic jumps of the Li^+ ions, the tip structure suddenly stabilizes. This is accompanied by a considerable drop in energy seen in figure 6 at about 19 Å and corresponds to formation of a quite regular structure of five LiF molecules on the tip shown in figure 5. From this point the Li^+ assumes the role of the last tip ion. To make sure that the tip structure has now stabilized completely, the direction of scanning was reversed as is indicated by the arrows in figure 6. Remarkably, the energy curves almost exactly repeat each other because the displacements of the tip and surface ions are strong but completely reversible.

Similar simulations were made for different tip heights and directions of scanning [80, 81]. They demonstrated that when the tip scans closer to the surface, which corresponds to increase of an average repulsive force up to 3 nN, similar behaviour persists: after some period of instability the cluster of surface material adjusts itself to new conditions of scanning and assumes a new stable structure. However, the new structure and 'probing atom' were different. When the tip load increases to approximately 3 nN, the tip–surface interaction becomes so invasive that the structure of the tip–surface junction cannot stabilize. Figure 7 provides an illuminating top view on the behaviour of the tip and the surface ions along the scan as the tip scans along the ⟨100⟩ surface axis [81]. The Li^+ ion at the end of the tip probes the space between two parallel lines of ions. Characteristic wiggles, which correlate with the energy behaviour, are due to the Coulomb repulsion from the surface Li^+ ions and attraction to the surface F^- ions.

These calculations demonstrated that the tip modification makes the tip–surface interaction less destructive; therefore this process was termed 'self-lubrication'. The dynamic self-organization of the surface material on the tip during scanning could be a general effect which may explain why periodic surface images are obtained with contaminated tips at relatively small tip loads of up to 3 nN. At larger repulsive forces, both modelling and experiment demonstrate a deterioration of the normal force image and surface wear.

Analysis of molecular dynamics reaffirms the conclusions of earlier static calculations that the surface image in contact mode is determined by the (periodic) interaction of many tip and surface ions (which includes the tip reconstruction and ion diffusion) and reflects the surface structure in a very indirect way. Even an atomically sharp tip probes simultaneously several surface rows (see figure 7) and the extremes of the force should not necessarily correspond to the average positions of the surface ions. The image may invert dependent on the tip chemical structure [78, 112]. These results imply that, unless one is able to control the tip position and achieve a soft approach to the surface without jump-to-contact, interpretation of SFM images in terms of rigid surface and single tip atom interacting with individual surface atoms does not have real basis. This point can be clearly seen in modelling the imaging of surface defects.

4.4. Modelling of contact SFM imaging of surface defects

The model which is emerging from these simulations is more of the interface between two flexible many-atom systems which constantly adjusts their structures as they move relative to each other, rather than of a single atom tip profiling a rigid or slightly deformable surface of individual ions. A strong adhesion of the surface atoms to the tip (and vice versa) and dynamic tip modification during scanning which in some conditions can promote periodic tip–surface interaction, could be destructive for defect imaging. This can be illustrated by comparing the results of modelling of step imaging on the NaCl surface. With a relatively inert diamond tip a sharp contrast in the step image was obtained in [79]. The calculations [112, 123] with the more adhesive MgO tip and with that modified by a dissociated water molecule demonstrated much stronger step deformation and also tip contamination by a cluster of the surface material as it scales the monatomic step. This implies that one should be very careful in choosing the tip material when trying to image and identify a point surface defect. For instance, an impurity ion can be easily picked up by the tip during scanning. Unfortunately, we must admit that presently there is not much choice in the tip materials available to the experimenter.

To illustrate our point further, it is instructive to discuss the results of modelling imaging of a non-periodic feature such as a point defect at the surface. Impurity Mg^{2+} ions compensated by cation vacancies are known to be stable at the LiF surface [78]. Modelling of the SFM imaging of this defect by the MgO tip contaminated by a stable cluster of the surface material scanning at different heights has been performed in [124] using the molecular dynamics technique.

Two normal force scanlines calculated for the tip moving at approximately 2.3 and 2.0 Å from the ideal surface plane are shown in figure 8. One can see that they are strongly perturbed in the middle where the tip is supposed to encounter the defect. In spite of a not very significant difference in the tip height, the characters of perturbations (which are the SFM defect images) and their origins are completely different. The trajectories of the tip and surface ions are shown in figure 9. They clearly demonstrate that at a larger tip–surface distance (figure 9(a)) the oxygen ion at the end of the tip first tried to adjust its position as it approached the impurity, but then the impurity Mg ion was kicked out of its original site exchanging places with the compensating cation vacancy. A much more dramatic picture emerges in figure 9(b). Here the tip was closer to the surface and one of the surface fluorine ions first adsorbed onto the tip, then another surface fluorine ion jumped into the vacancy. The vacancy of the second fluorine was promptly occupied by the third fluorine ion along the tip trajectory which jumped into it, as can be seen on the trajectory plot in figure 9(b). Its place was occupied by the tip oxygen ion which made a bond with the impurity and stayed at the surface. Interestingly, when the tip was scanning back along the same line, a back exchange by another route took place and the oxygen ion has returned back to the tip, which is reflected in completely different profiles of the forward and backward scanlines in figure 8(b).

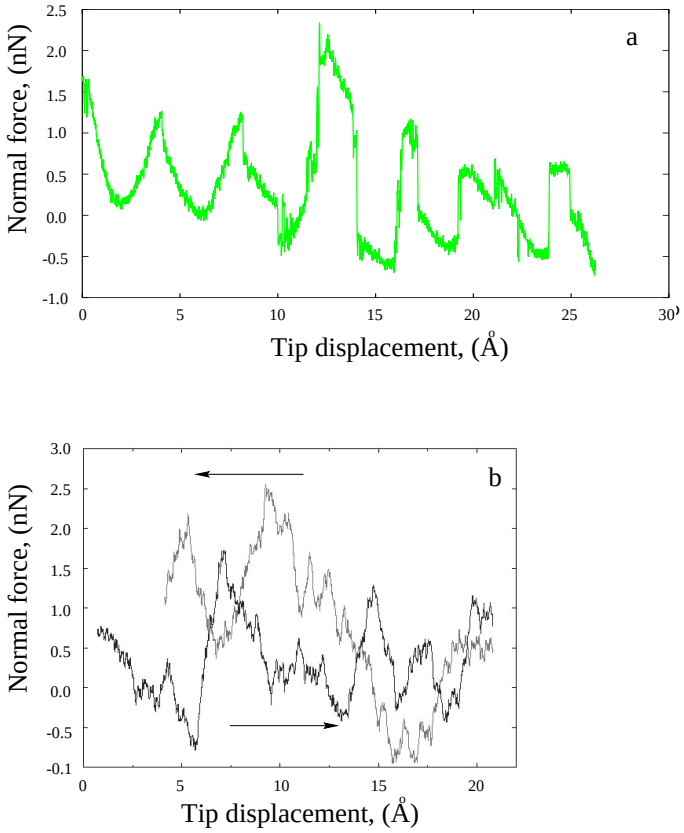

Figure 8. The normal force on the tip against tip position for constant speed tip motion at constant height above the LiF surface with the Mg^{2+}–cation vacancy defect calculated using the molecular dynamics technique for the tip height about 2.3 Å (a) and 2.0 Å (b) above the surface; (b) shows the scanline in the forward and backward directions. Note more regular force behaviour at larger tip–surface distance and different response to the defect at different tip heights and scan directions.

These calculations demonstrate that the scanlines reflect the effect of perturbation of the tip–surface interaction by the defect rather than the defect structure. The defect image is constructed from many such scanlines, but each of them may correspond to completely different defect structure, which can explain why impurities are so difficult to observe experimentally even in specially doped samples.

To summarize, our modelling of the contact SFM reveals a complex mechanism of contrast formation and implies that the interpretation of even periodic surface images in terms of the chemical identity of the extremes visible in the image is difficult and depends on the unknown tip structure. Therefore the so called non-contact or dynamic mode of SFM imaging seems to offer a better alternative to achieve atomic resolution. However, it has its own problems which are discussed below.

4.5. Modelling of non-contact mode

A different approach to SFM imaging introduced 12 years ago [125] suggests avoiding the tip–surface contact altogether and to measure changes in vibrational properties of the cantilever

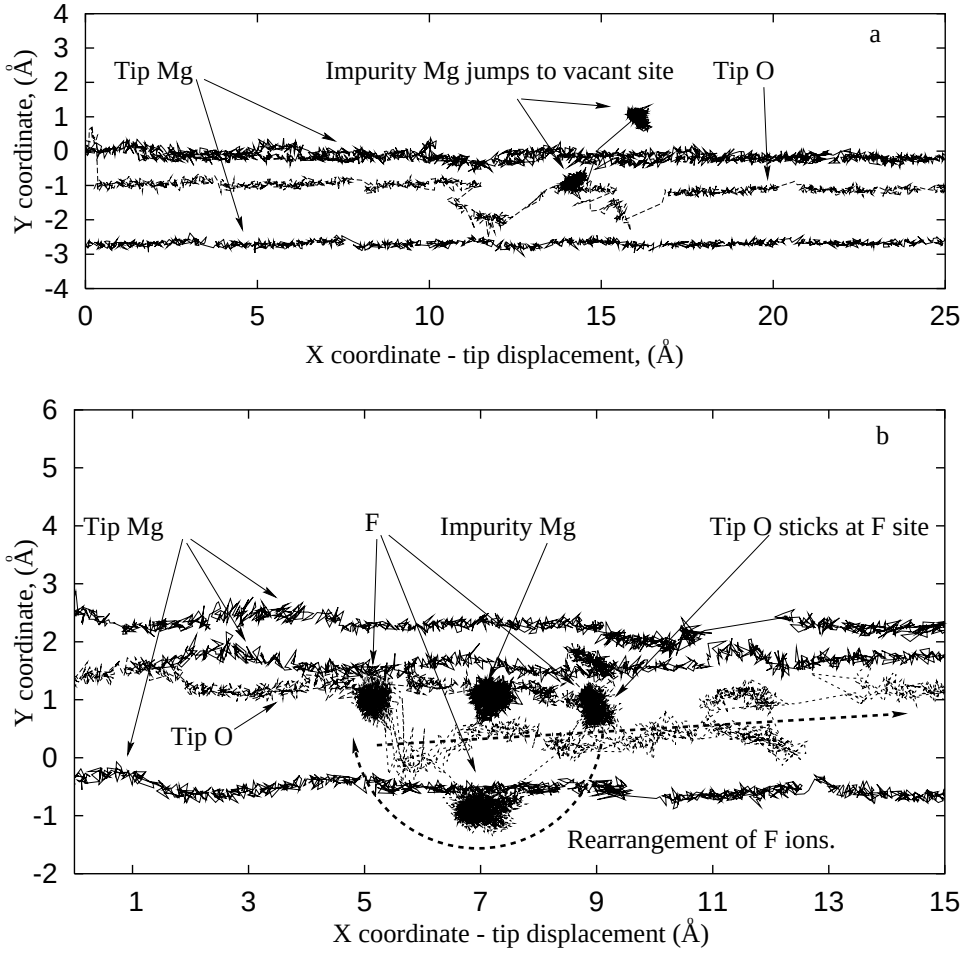

Figure 9. The top view of the trajectories of some of the tip and surface ions during constant speed tip motion at constant height above the LiF surface with the Mg^{2+}–cation vacancy defect calculated using the molecular dynamics technique for the tip height about 2.3 Å (a) and 2.0 Å (b) above the surface. The tip is moving from left to right. Note the defect and tip transformations caused by their interaction.

induced by tip–sample interaction. In this mode, the SFM tip oscillates and its interaction with the surface changes the parameters of these oscillations. In most cases frequency modulation is used [126] where a cantilever is subject to positive feedback such that it oscillates with constant amplitude, A_0. The best performance in this mode is achieved if the tip does not enter the repulsive part of the interaction and periodically moves in and out of the short-range interaction region. Very recently, several authors have reported atomic resolution in this mode first on Si surfaces [7, 8] and then on other surfaces including alkali halides [41, 42] and TiO_2 [57–59].

In most experimental set-ups of NC-SFM in UHV a cantilever vibrates at its resonance frequency, f_0 (about 150–200 KHz), and with large amplitude (100–200 Å). The system usually has a very large quality factor in the range of 15 000–20 000 [41] or even 38 000 [9, 127]. When the sample is brought sufficiently close that the tip is beginning to sense the interaction with

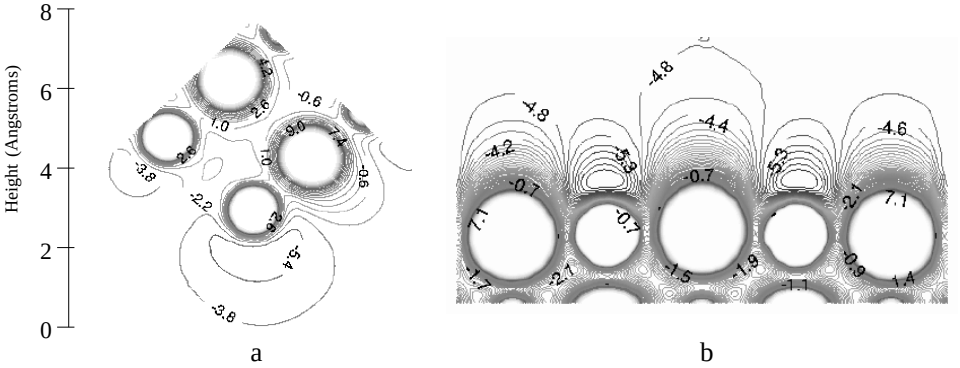

Figure 10. Sections of the electrostatic potential (in eV) produced by the $(MgO)_{32}$ cube tip (a), and by the MgO surface with one Mg ion displaced by 0.15 Å out from the surface (b). The tip potential is shown in the plane which includes the ⟨111⟩ cube axis through the oxygen tip ion.

the surface, the frequency and amplitude of the oscillations change. At small perturbations, and with frequency modulation keeping A_0 constant, this may be characterized by a shift in the resonant frequency, Δf. Hence a combination of parameters f_0, Δf, k and the amplitude of cantilever oscillations A_0 determines the cantilever oscillations. Assuming an inverse power and exponential dependence of the tip–surface forces, Giessibl [29, 108] performed a thorough analysis of NC-SFM operation using perturbation theory. He derived the analytical expressions for Δf as a function of the tip oscillations and force parameters, and also obtained the optimal set of parameters f_0, k, A_0 for NC-SFM operation as a function of the tip–sample potential. Image acquisition in NC-SFM is achieved by scanning of the cantilever across the sample in the xy plane and adjusting the equilibrium position of the cantilever, h, with respect to the surface plane such that f (hence Δf) is constant. This yields a map $h(x, y, \Delta f, A_0)$ which, taking into account the thermal noise [29, 108], provides the surface image. Hence, in order to simulate a real NC-SFM image one needs to know the tip–surface interaction force-field $\boldsymbol{F}(x, y, z)$. For model tips it can be calculated using the molecular dynamics, or static atomistic simulation and quantum mechanical techniques [83, 93, 94]. Then surface images $h^{theor}(x, y, \Delta f, A_0)$ corresponding to different constant frequency shifts Δf can be constructed using the analytical expressions [29, 108] or a numerical procedure [94], and compared with experiment.

4.6. Non-contact mode SFM images and contrast mechanisms

The first complete set of such calculations which attained the theoretical NC-SFM images of MgO, NaCl and LiF surfaces was performed in [83] and [94]. The constant frequency shift images were obtained using the force fields $\boldsymbol{F}(x, y, z)$ calculated by atomistic simulation techniques for different orientations of the MgO tip to the surface. As discussed in [83] and [94], the contrast in calculated images is determined by an interplay of the electrostatic and van der Waals forces. In the case of both insulator tip and surface, the main contributions to the contrast formation result from the interaction of the tip with the alternating surface potential and with the surface polarization induced by the electric field of the tip. The electrostatic potential of the MgO tip is shown in figure 10. If the tip is turned by its oxygen corner to e.g. the MgO surface, it attracts the Mg ions, which displace towards the tip, and repels the oxygen ions displacing them into the surface. Both displacements produce dipole moments which interact with the tip potential. The electrostatic potential of the MgO surface with one Mg ion

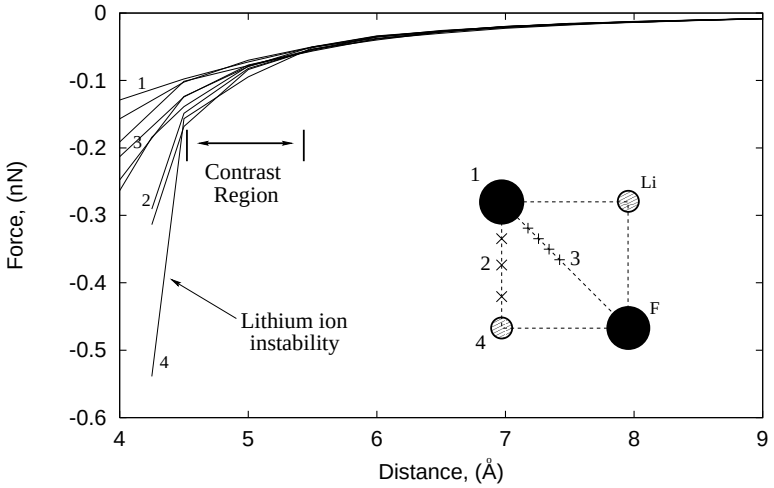

Figure 11. The force–distance curves calculated above nine different positions (shown in the inset) of the LiF surface with the MgO nano-tip using the molecular dynamics technique.

displaced outwards by 0.15 Å is also shown in figure 10. It was calculated using the same *ab initio* density functional technique as was used in the tip calculations discussed in section 4.1. One can see that, due to low coordination and high ionicity, the tip produces a strong localized potential which extends over several ångströms. The dipole potential of the displaced ion decays much more slowly than the exponentially decaying electrostatic potential of the ideal surface. Displacing ions outside the surface is easier than inside. Outward displacement also increases the attraction due to the reduced distance to the tip. Therefore the interaction of the tip with the induced lattice polarization above the cation and anion sites is different, which strongly contributes to the image contrast. If the tip moves closer, this finally leads to instability and strong displacement of the Li, Na or Mg ions, discussed in [118]. In the case of LiF, this can be seen as the onset of strong attraction in the force curves in figure 11. These curves were calculated above nine different surface points in order to produce the surface image. The distance range between the instability region and the place where the curves split, marked in figure 11, determines the range of tip–surface separations where one can expect some contrast in the image due to the chemical forces. One can see that for LiF this range is quite narrow, between about 4.4 and 5.4 Å.

The effect of the tip-induced surface deformation is also illustrated in figure 12, which shows the displacements of the surface Na ions at two positions of the MgO tip above the NaCl surface. One can see that a 'blunter' tip used in these calculations causes strong displacements of both cation and anion attracted to the oxygen and magnesium ions on the tip. Since MgO is much harder than both LiF and NaCl, the displacements of the MgO surface ions due to the interaction with the MgO tip are much smaller. However, the ionic charges are twice as large and on balance the tip–surface interaction is not much different from that for LiF and NaCl. This discussion applies equally to the tip ions. However, their displacements in our case are much smaller than e.g. those for the softer NaCl surface.

Polarization of the surface ions by the electric field of the tip also contributes to the image contrast due to the different polarizability of cations and anions. This effect is accounted for in static atomistic modelling for NaCl and MgO [83], but it is relatively small due to the small ion polarizabilities in these systems. Another factor which affects the contrast is the relation between the surface interionic spacing and the effective diameter of the region where the tip has

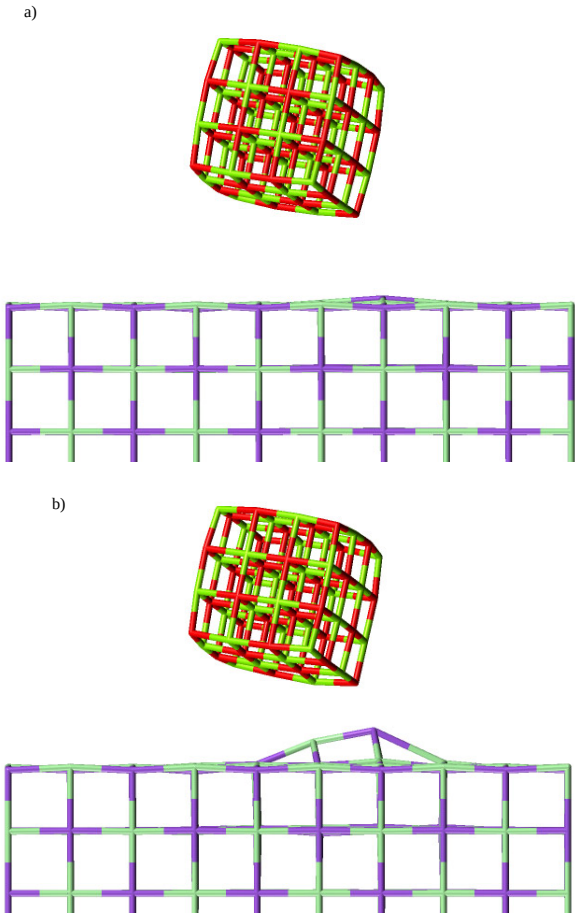

Figure 12. The snapshot configurations of the MgO nano-tip interacting with the NaCl surface. (a) corresponds to the tip–surface distance about 4.2 Å just before, and (b) to the distance 4.1 Å and the configuration just after the instability of the surface Na ion has occurred. Note the strong displacements of the surface ions in both cases.

a strong electric field gradient probing the surface (see figures 4 and 10). Roughly speaking, the tip can 'resolve' the surface ions better if they are further apart.

It is known that an attractive tip–surface interaction decreases the frequency of cantilever oscillations whereas a repulsive interaction makes it bigger than f_0. Therefore, in the presence of repulsion there is a maximum frequency shift $(\Delta f)_{max}$ corresponding to the maximum attraction before the frequency starts to increase thus decreasing Δf. To estimate the maximum scanline corrugation at given cantilever and interaction parameters, the scanlines for the NaCl surface at the frequency change $(\Delta f)_{max}$ for three different effective tip radii were calculated in [83] using the same setup as shown in figure 1. We remind the reader that the main contribution to the van der Waals interaction in this model is provided by that between the tip sphere and the semi-infinite surface. The maxima in the scanlines shown in figure 13 correspond to the areas of the strongest tip–surface attraction. One can see that as the van der Waals interaction increases (proportional to the tip radius R), $(\Delta f)_{max}$ becomes bigger and the tip moves closer to the surface which results in the increase in scanline corrugation. This results from the fact

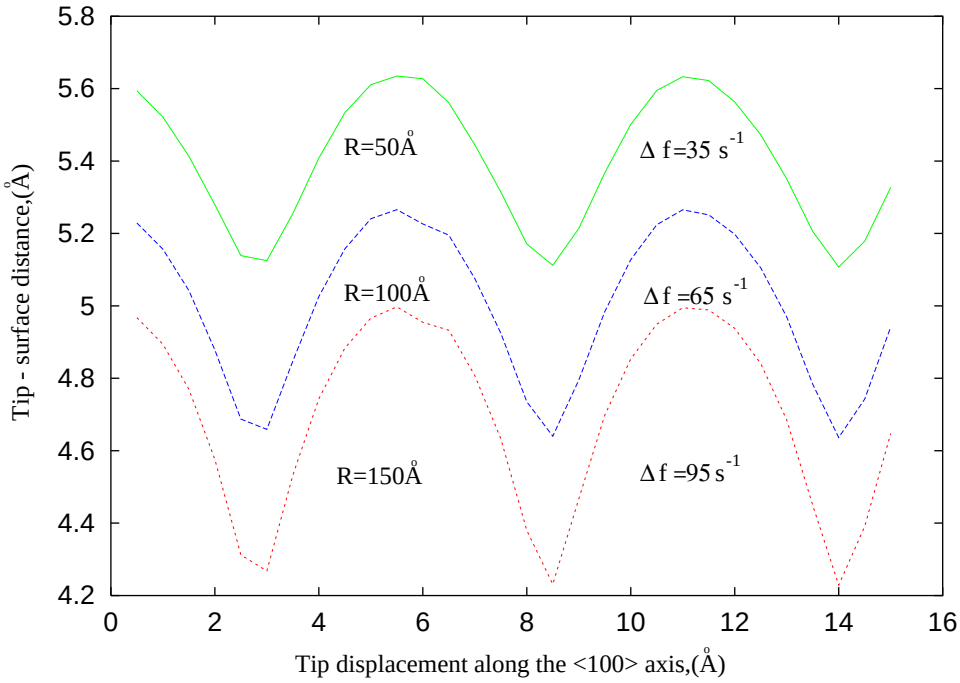

Figure 13. Scanlines calculated at different tip radii for the maximum frequency shift obtained for the MgO tip interaction with the NaCl surface.

that corrugation is determined by the relative changes of the force in the lateral direction. As the van der Waals interaction increases, the relative changes of the force at the same tip height, determined by the chemical contribution, decrease. Therefore the tip should move closer to the surface where the split of the force curves is larger; this increases both the scanline corrugation and the frequency shift. In other words, sharp tips are better both in terms of sensitivity and stability of NC-SFM operation because they provide contrast at larger tip–surface distances.

Similar calculations, using the MgO tip and the atomistic simulation technique, have recently been performed in our group for the (110) TiO_2 surface. They demonstrated that the short-range interaction of the oxygen terminated tip is stronger with the titanium rows (see figure 2). Therefore these calculations predict the titanium rows to be seen as 'bright' and bridging oxygen rows as 'dark' in the NC-SFM images [57].

How can one test these predictions against experiment? The predicted image corrugations are in good agreement with the experimental data [42], which supports the proposed mechanism of image contrast. The results demonstrate that for the tip models used in [83] and [94] the extremes in the calculated images, which should correspond to 'bright' and 'dark' spots in experimental images, are located at average positions of surface ions. However, we should note that the contrast will invert if the tip probes the surface not by the oxygen ion but by a positive low-coordinated ion. Therefore, unless the tip apex structure is established, the chemical identity of the image features is impossible to prove, and, for instance, whether our results for TiO_2 contradict the mechanistic interpretation suggested in [59] is unclear. A way forward would be to 'mark' one type of surface ion by adsorbing atoms or molecules. Then comparison of experimental and theoretical 'images' of the adsorbed species could allow resolution of the surface chemical structure, and provide some information regarding the tip

structure. However, as demonstrated by Fukui *et al* [58], this still remains one of the challenges for experimental techniques.

The contrast mechanisms of NC-SFM on semiconductors such as Si and InP should take into account the covalent nature of chemical bonding in these materials. The calculations [93] demonstrated that the onset of chemical bonding between a dangling bond localized at the end of the silicon tip and the dangling bonds on the adatoms of the Si(111) surface could contribute to the contrast formation. The analysis of the NC-SFM image of Si(111) made in [105] led the authors to suggest that the image contrast could be due to variations in the relaxation of the outermost surface atoms due to their interaction with the tip. Thus the contribution of the relaxation of surface atoms to NC-SFM image contrast seems to be a general effect. However, the impact of the tip–surface chemical bonding is much more difficult to prove, again due to the unknown detailed chemical structure of the tip apex. As discussed above, the likely contamination of the Si tip by residual water or oxygen can affect significantly the character of the tip–surface interaction, and hence the mechanism of image contrast.

Another problem, which was just indicated in the context of NC-SFM, concerns the possibility of tip contamination by the surface material. This may be caused, in particular, by the instabilities of the surface ions and by their adsorption onto the tip. This in turn affects the tip–surface interaction. Model calculations show that the character of the cantilever oscillations may become very complicated and even unstable if the perturbation due to the tip–surface interaction is too large. Most of the experimental papers admit that NC-SFM is prone to instabilities, resulting in tip contamination due to contact with the surface [9, 42, 105]. Therefore in the next section we discuss how the NC-SFM instabilities can be related to the tip contamination.

4.7. Role of avalanche adhesion in stability of NC-SFM operation

As discussed in the previous section, to be able to resolve different ions the smallest tip–surface separation should be comparable to the interatomic distance. At such distances an avalanche adhesion of the surface ions on the tip (and vice versa) may become important. This effect is similar to avalanche adhesion of solid surfaces which was first demonstrated for metals [128]. Its mechanism for metallic tips and surfaces was considered in [14], [91], [120], [129] and [131]. For ionic materials it was discussed in [118]. The occurrence of instabilities of the surface and tip ions or atoms strongly depends on the tip and surface chemical structure and the tip–surface distance: for some pairs of materials and for the tip–surface distances exceeding the critical distance these instabilities may not occur. Roughly speaking, an inert tip which does not produce a strong local electric field and has weak adhesion to the surface ions may not induce instability. But it is also difficult to expect a good image contrast with such a tip. The tip with opposite qualities may provide better contrast, but is more difficult to operate.

The instabilities of the tip and surface ions can be relevant to our discussion of NC-SFM operation in two ways. First, the instability means that at some critical tip–surface distance the surface ions strongly displace from their sites (see figure 12) causing an abrupt change in the tip–surface interaction [78, 129, 132]. Although the change in the force due to this effect may be often just 0.3–1.0 nN (see, for example, figure 11), the force gradient is of the order of 10–30 N m^{-1}. Secondly, if this or a smaller tip–surface distance is the turning point of the tip oscillations, some ions may be trapped by the tip, changing the tip–surface interaction even more. The assumption of the stationary force-field $\boldsymbol{F}(\boldsymbol{r})$ may become invalid if the frequency of these tip modifications is comparable with the period of cantilever oscillations, and these oscillations may become very complex. Moreover, as was demonstrated in [118], the initial tip and surface modification may lead to neck formation and therefore to much more severe changes

in the tip–surface interaction. We should also note that the effect depends on the charge state of the adsorbed species: adsorption in ionic form charges the tip and the surface and induces more significant changes in the interaction. Can this affect the cantilever oscillations in any significant way? To answer this question, the effect of the MgO tip contamination due to the interaction with the LiF surface on the parameters of cantilever oscillations was studied in [94]. The calculations demonstrated that both the change in the interaction due to the tip-induced instability of Li ions at the surface and adsorption of one ion on the tip are not likely to cause significant perturbation in the cantilever oscillations. They suggest that a more likely scenario could be that the initial tip contamination can develop into a neck formation or adsorption of a cluster of the surface material onto the tip, which can eventually lead to a tip crash into the surface.

One can look at these results also from a different perspective. New experimental techniques such as NC-SFM are sensitive to even tiny variations of tip–surface forces and may allow us to single out elementary processes which have previously been masked by the jump-to-contact and jump-off tip instabilities, and to correlate them with the atomic structure and other properties of surfaces near contact. In particular, tip–surface transfer of atoms is important for SFM manipulation of atoms and molecules and construction of new nanostructures. Novel phenomena which may soon become possible to study with SFM include quantum oscillations of atoms between tip and surface [121], and electronic effects due to the tip–surface interaction [133].

5. Discussion

The above analysis of the experimental and theoretical data demonstrates that in spite of quite extensive theoretical studies a gap still exists between theoretical modelling of SFM and experimental images. It would be fair to say that there is no experimental image which would be fully explained by atomistic modelling, although some comparisons were made. The main reason is the unknown tip structure. The results presented in this paper reveal that atomistic modelling can be used in order to develop a detailed picture of the tip–surface interaction and contrast formation. It has already predicted effects which go beyond our intuitive understanding of the SFM imaging. However, quantitative simulation of experimental images similar to that common in EPR, EXAFS and other spectroscopies is still impossible. On the other hand, taking into account the rapidly growing number of experimental images, it would be unrealistic to hope that such quantitative analysis would be possible in each case and indeed impractical to make it. Good working models are needed for this purpose.

In our discussion we focused on the interaction of hard oxide tips with softer surfaces, such as alkali halides, in UHV, which is a prototype situation in many experiments. What do these results contribute to the building of a model of the SFM imaging of insulators? In general terms, they demonstrate that the tip–surface interaction during scanning in hard contact involves dynamic tip and surface reorganization and surface deformation which at small tip loads may promote periodic overall force on the tip, but generally leads to tip and surface wear. There seems to be little chance that point defects can be reliably and reproducibly imaged in hard contact. Therefore we can conclude that conventional contact mode SFM is too invasive and does not allow reliable and routine interpretation; this makes atomic resolution in contact SFM virtually impossible.

Although the non-contact mode is definitely a step forward in terms of both imaging and interpretation, its implementation has proved to be very difficult due to the very narrow region of stable operation; it will be also difficult to use for surface modification and atom manipulation. The ionic displacements from the original surface sites and their instabilities

at the surface due to the interaction with the tip significantly affect the contrast formation and stability of non-contact SFM imaging. Tailoring the tip material and structure to observe particular surface properties and defect structures is becoming an important issue. One of the shortcomings of SFM is that all the information about the system is contained in the force measurements which are then transformed into a structural image. Combination of non-contact SFM with STM [57] on thin insulating (especially oxide) films provides a possibility to obtain more information about the system and make the interpretation of the results more reliable. However, this would require use of conductive tips in both experiments, which complicates the modelling because of a very significant contribution of the image force. Our estimates of the relative role of different forces in the case of the interaction of metallic tips with the TiO_2 surface demonstrate that the image force can be much stronger than even the van der Waals force.

What would then be an 'ideal' SFM which would allow reliable image interpretation and manipulation of atoms at the surface? It should provide a constant contact between a well defined tip and a surface, be able to control the tip–surface separation and surface perturbation and measure very small forces or force gradients. Although this may seem rather unrealistic, recent advances in the SFM instrumentation [134], which allow one to control the tip position using a small magnet attached to it, can make a softer approach more routine. Development of new cantilevers, controlled tip modification, low-temperature and variable-temperature SFM will soon make this technique as widely used for atomic scale imaging and analysis as it is now for the studies of surface properties on nano- and microscales.

Acknowledgments

AIL and ASF are supported by EPSRC. The authors are grateful to F Giessibl, and R Bennewitz, E Meyer, A Baratoff and all members of the Basel SPM group for very useful and stimulating discussions on NC-SFM and to G Thornton and H Raza for illuminating comments on applications of NC-SFM to oxides. We would like to thank J Gavartin for introducing us to the world of Si clusters, R Pérez for providing the LDA optimized structure of the Si(111) (5×5) reconstruction, and P Sushko and L Kantorovich for help in calculations and many useful discussions. We are grateful for an allocation of time on Cray T3E at EPCC provided by the High Performance Computing Initiative through the Materials Chemistry consortium.

References

[1] Güntherodt H-J, Anselmetti D and Meyer E (eds) 1995 *Forces in Scanning Probe Methods (NATO ASI Series E 286)* (Dordrecht: Kluwer)
[2] Carpick R W and Salmeron M 1997 *Chem. Rev.* **97** 1163
[3] Meyer E, Overney R, Dransfeld K and Gyalog T 1999 *Nanoscience: Friction and Rheology on the Nanometer Scale* (Singapore: World Scientific)
[4] Jandt K D 1998 *Mater. Sci. Eng. Rep.* **21** 221
[5] Gruverman A, Auciello O and Tokumoto H 1998 *Integrated Ferroelectr.* **19** 49
[6] Giessibl F J 1994 *Japan. J. Appl. Phys.* **33** 3726
[7] Giessibl F J 1995 *Science* **267** 68
[8] Lüthi R, Meyer E, Bammerlin M, Baratoff A, Lehmann T, Howald L, Gerber C and Güntherodt H-J 1996 *Z. Phys.* B **100** 165
[9] Sugawara Y, Ohta M, Ueyama H, Morita S, Osaka F, Ohkouchi S, Suzuki M and Mishima S 1996 *J. Vac. Sci. Technol.* B **14** 953
[10] RosaZeiser A, Weilandt E, Hild S and Marti O 1997 *Meas. Sci. Technol.* **8** 1333
[11] Jarvis S P, Yamamoto S I, Yamada H, Tokumoto H and Pethica J B 1997 *Appl. Phys. Lett.* **70** 2238
[12] Allers W, Schwarz A, Schwarz U D and Wiesendanger R 1998 *Rev. Sci. Instrum.* **69** 221

[13] Li F B, Thompson G E and Newman R C 1998 *Appl. Surf. Sci.* **126** 21
[14] Landman U, Luedtke W D, Burnham N A and Colton R J 1990 *Science* **248** 454
[15] Burnham N A, Colton R J and Pollock H M 1993 *Nanotechnology* **4** 64
[16] Marti O and Colchero J 1995 *Forces in Scanning Probe Methods (NATO ASI Series E 286)* ed H-J Güntherodt, D Anselmetti and E Meyer (Dordrecht: Kluwer) p 15
[17] Castle J E and Zhdan P A 1997 *J. Phys. D: Appl. Phys.* **30** 722
[18] Israelachvili J N 1991 *Intermolecular and Surface Forces* 2nd edn (London: Academic)
[19] Hamaker H C 1937 *Physica* **4** 1058
[20] Lifshitz E M 1956 *Sov. Phys.-JETP* **2** 73
[21] Hartmann U 1990 *Phys. Rev.* B **42** 1541
[22] Goodman F O and Garcia N 1991 *Phys. Rev.* B **43** 4728
[23] Garcia N and Binh V T 1992 *Phys. Rev.* B **46** 7946
[24] Jarvis S P and Pethica J B 1995 *Forces in Scanning Probe Methods (NATO ASI Series E 286)* ed H-J Güntherodt, D Anselmetti and E Meyer (Dordrecht: Kluwer) p 105
[25] Petrenko V F 1997 *J. Phys. C: Solid State Phys.* **101** 6276
[26] Marti O, Drake B and Hansma P K 1987 *Appl. Phys. Lett.* **51** 484
[27] Weisenhorn A L, Maivald P, Butt H-J and Hansma P K 1992 *Phys. Rev.* B **45** 11 226
[28] Hutter J L and Bechhoefer J 1993 *J. Appl. Phys.* **73** 4123
[29] Giessibl F J 1997 *Phys. Rev.* B **56** 16 010
[30] Tersoff J and Hamann D R 1985 *Phys. Rev.* B **31** 805
[31] Meyer E, Heinzelmann H, Brodbeck D, Overney G, Overney R, Howald L, Hug H, Jung T, Hidber H-R and Güntherodt H-J 1991 *J. Vac. Sci. Technol.* B **9** 1329
[32] Dietz P, Ramos C A and Hansma P K 1992 *J. Vac. Sci. Technol.* B **10** 741
[33] Perrot E, Dayez M, Humbert A, Marti O, Chapon C and Henry C R 1994 *Europhys. Lett.* **26** 659
[34] Ikemiya N, Kitamura A and Hara S 1996 *J. Crystal Growth* **160** 104
[35] Giessibl F J and Binnig G 1992 *Ultramicroscopy* **42–44** 281
[36] Shluger A L, Wilson R M and Williams R T 1994 *Phys. Rev.* B **49** 4915
[37] Xu L, Bluhm H and Salmeron M 1998 *Surf. Sci.* **407** 251
[38] Gelb L D and Lynden-Bell R M 194 *Phys. Rev.* B **49** 2058
[39] Patrick D L and Lynden-Bell R M 1997 *Surf. Sci.* **380** 224
[40] Meyer G and Amer N A 1990 *Appl. Phys. Lett.* **57** 2089
[41] Bammerlin M, Lüthi R, Meyer E, Baratoff A, Lu J, Guggisberg M, Gerber C, Howald L and Güntherodt H-J 1997 *Probe Microsc.* **1** 3
[42] Bammerlin M, Lüthi R, Meyer E, Baratoff A, Guggisberg M, Loppacher C, Lu J, Gerber C and Güntherodt H-J 1998 *Appl. Phys.* A **66** S293
[43] Heinzelmann H, Mayer E, Brodbeck D, Overney G and Güntherodt H-J 1992 *Z. Phys.* B **88** 321
[44] Overney R M, Haefke H, Meyer E and Güntherodt H-J 1992 *Surf. Sci. Lett.* **277** L29
[45] Meyer E, Heinzelmann H, Grütter P, Hidber H-R and Güntherodt H-J 1989 *J. Appl. Phys.* **66** 4243
[46] Heinzelmann H, Meyer E, Güntherodt H-J and Steiger R 1989 *Surf. Sci.* **221** 1
[47] Barrett R C and Quate C F 1990 *J. Vac. Sci. Technol.* A **8** 400
[48] Sum R, Lang H P and Güntherodt H-J 1995 *Physica* C **242** 174
[49] Shindo H and Nozoye H 1992 *J. Chem. Soc. Faraday Trans.* **88** 711
[50] Shindo H and Nozoye H 1993 *Surf. Sci.* **287/288** 1030
[51] Smith R L, Rohrer G S, Lee K S, Seo D-K and Whangbo M-H 1996 *Surf. Sci.* **367** 87
[52] Komiyama M and Yashima T 1994 *Japan. J. Appl. Phys.* **33** 3761
[53] Meyer G and Amer N M 1990 *Appl. Phys. Lett.* **56** 2100
[54] Ohta M, Konishi T, Sugawara Y, Morita S, Suzuki M and Enomoto Y 1993 *Japan. J. Appl. Phys.* **32** 2980
[55] Howald L, Haefke H, Lüthi R, Mayer E, Gerth G, Rudin H and Güntherodt H-J 1994 *Phys. Rev.* B **49** 5615
[56] Sugawara Y, Ohta M, Hontani K, Morita S, Osaka F, Ohkouchi S, Suzuki M, Nagaoka H, Mishima S and Okada T 1994 *Japan. J. Appl. Phys.* **33** 3739
[57] Fukui K, Onishi H and Iwasawa Y 1997 *Phys. Rev. Lett.* **79** 4202
[58] Fukui K, Onishi H and Iwasawa Y 1997 *Chem. Phys. Lett.* **280** 296
[59] Iwasawa Y 1998 *Surf. Sci.* **402–404** 8
[60] Bennewitz R, Bammerlin M, Loppacher C, Guggisberg M, Eng L, Meyer E, Güntherodt H-J, An C P and Luty F 1999 *Radiat. Eff. Defects Solids* at press
[61] Henrich V E 1985 *Rep. Prog. Phys.* **48** 1481
[62] Charlton G, Howes P B, Nicklin C L, Steadman P, Taylor J S G, Muryn C A, Harte S P, Mercer J, McGrath R, Norman D, Turner T S and Thornton G 1997 *Phys. Rev. Lett.* **78** 495
[63] Maschhoff B L, Pan J-M and Madey T E 1991 *Surf. Sci.* **259** 190

[64] Murray P W, Condon N G and Thornton G 1995 *Phys. Rev.* B **51** 989
[65] Sander M and Engel T 1994 *Surf. Sci.* **302** L263
[66] Onishi H and Iwasawa Y 1994 *Surf. Sci.* **313** L783
[67] Purton J, Bullett D W, Oliver P M and Parker S C 1995 *Surf. Sci.* **336** 166
[68] Ramamoorthy M, Vanderbilt D and King-Smith R D 1994 *Phys. Rev.* B **49** 16 721
[69] Lindan P J D, Harrison N M, Gillan M J and White J A 1997 *Phys. Rev.* B **55** 15 919
[70] Oliver P M, Watson G W, Kelsey E T and Parker S C 1997 *J. Mater. Chem.* **7** 563
[71] Zonnchen P, Thiele G, Hess C, Schlenker C, Bengel H, Cantow H-J, Magonov S N, Seo D-K and Whangbo M-H 1996 *New J. Chem.* **20** 295
[72] Van Labeke D, Labani B and Girard C 1989 *Chem. Phys. Lett.* **162** 399
[73] Giessibl F J 1992 *Phys. Rev.* B **45** 13 815
[74] Shluger A L, Pisani C, Roetti C and Orlando R 1990 *J. Vac. Sci. and Technol.* A **8** 3967
[75] Ciraci S, Baratoff A and Batra I P 1990 *Phys. Rev.* B **41** 2763
[76] Tekman E and Ciraci S 1991 *J. Phys.: Condens. Matter* **3** 2613
[77] Tang H, Joachim C, Devillers J and Girard C 1994 *Europhys. Lett.* **27** 383
[78] Shluger A L, Rohl A L, Gay D H and Williams R T 1994 *J. Phys.: Condens. Matter* **6** 1825
[79] Tang H, Bouju X, Joachim C, Girard C and Devillers J 1998 *J. Chem. Phys.* **108** 359
[80] Livshits A I and Shluger A L 1997 *Faraday Discuss.* **106** 425
[81] Livshits A I and Shluger A L 1997 *Phys. Rev.* B **56** 12 482
[82] Krüger D, Anczykowski B and Fuchs H 1997 *Ann. Phys., Lpz.* **6** 341
[83] Livshits A I, Shluger A L and Rohl A L 1999 *Appl. Surf. Sci.* **140** 327
[84] Gleyzes P, Kuo P K and Boccara A C 1991 *Appl. Phys. Lett.* **58** 2989
[85] Winkler R G, Spatz J P, Sheiko S, Moller M, Reineker P and Marti O 1996 *Phys. Rev.* B **54** 8908
[86] Burnham N A, Behrend O P, Oulevey F, Gremaud G, Gallo P-J, Gourdon D, Dupas E, Kulik A J, Pollock H M and Briggs G A D 1997 *Nanotechnology* **8** 67
[87] Sasaki N, Tsukada M, Tamura R, Abe K and Sato N 1998 *Appl. Phys.* A **66** S287
[88] Tsukada M, Sasaki N, Yamura R, Sato N and Abe K 1998 *Surf. Sci.* **401** 355
[89] Sasaki N and Tsukada M 1999 *Appl. Surf. Sci.* **140** 339
[90] Giessibl F J, Bielefeldt H, Hambacher S and Mannhart J 1999 *Appl. Surf. Sci.* **140** 352
[91] Ciraci S, Tekman E and Baratoff A 1992 *Phys. Rev.* B **46** 10 411
[92] Hartmann U 1994 *Adv. Electron. Electron Phys.* **87** 49
[93] Pérez R, Payne M C, Stich I and Terakura K 1997 *Phys. Rev. Lett.* **78** 678
[94] Livshits A I, Shluger A L, Rohl A L and Foster A S 1999 *Phys. Rev.* B **59** 2436
[95] Reiss G, Buckel H, Vancea J, Lecheler R and Hastreiter E 1991 *J. Appl. Phys.* **70** 523
[96] Grigg D A, Russell P E, Giffith J E, Vasile M J and Fitzgerald E A 1992 *Ultramicroscopy* **42–44** 1616
[97] Sheiko S S, Moller M, Reuvekamp E M C M and Zandbergen H W 1993 *Phys. Rev.* B **48** 5675
[98] Odin C, Aime J P, Kaakour Z E and Bouhacina T 1994 *Surf. Sci.* **317** 321
[99] Atamny F and Baiker A 1995 *Surf. Sci.* **323** L314
[100] Montelius L, Tegenfeldt J O and van Heeren P 1994 *J. Vac. Sci. Technol.* B **12** 2222
[101] Lantz M A, O'Shea S J and Welland M E 1998 *Rev. Sci. Instrum.* **69** 1757
[102] Argento C and French R H 1996 *J. Appl. Phys.* **80** 6081
[103] Shluger A L, Rohl A L, Gay D H and Williams R T *Forces in Scanning Probe Methods (NATO ASI Series E 286)* ed H-J Güntherodt, D Anselmetti and E Meyer (Dordrecht: Kluwer) p 169
[104] Tang H, Joachim C and Devillers J 1995 *Europhys. Lett.* **30** 289
[105] Erlandsson R, Olsson L and Mårtensson P 1996 *Phys. Rev.* B **54** R8309
[106] Bhushan B and Sundararajan S 1998 *Acta Mater.* **46** 3793
[107] Cross G, Schirmeisen A, Stalder A, Grutter P, Tschudy M and Durig U 1998 *Phys. Rev. Lett.* **80** 4685
[108] Giessibl F J 1999 *Scanning Microsc.* at press
[109] Sinnott S B, Colton R J, White C T and Brenner D W 1994 *Surf. Sci.* **316** L1055
[110] Sasaki N and Tsukada M 1995 *Japan. J. Appl. Phys.* **34** 3319
[111] Tsujimichi K, Tamura H, Hirotani A, Kubo M, Komiyama M and Miyamoto A 1997 *J. Phys. Chem.* B **101** 4260
[112] Shluger A L, Rohl A L, Williams R T and Wilson R M 1995 *Phys. Rev.* B **52** 11 398
[113] Sushko P V, Foster A S, Kantorovich L N and Shluger A L 1999 *Appl. Surf. Sci.* at press
[114] Kaxiras E 1990 *Phys. Rev. Lett.* **64** 551
[115] Takayanagi K, Tanishiro Y, Takahashi M and Takahashi S 1981 *J. Vac. Sci. Technol.* A **3** 1502
[116] Pancey C, Rochet F, Dufour G, Roulet A, Sirotti F and Panaccione E 1995 *Surf. Sci.* **338** 143
[117] Zaibi M A, Lacharme J P and Sebenne C A 1997 *Surf. Sci.* **377** 639
[118] Shluger A L, Kantorovich L N, Livshits A I and Gillan M J 1997 *Phys. Rev.* B **56** 15 332

[119] Zhong W and Tomanek D 1990 *Phys. Rev. Lett.* **64** 3054
[120] Sørensen M R, Jacobsen K W and Jónsson H 1996 *Phys. Rev. Lett.* **77** 5067
[121] Tilinin I S, Hove M A V and Salmeron M 1998 *Appl. Surf. Sci.* **130–132** 676
[122] Malghan S G 1992 *Colloids Surf.* **62** 87
[123] Shluger A L, Rohl A L, Wilson R M and Williams R T 1995 *J. Vac. Sci. Technol.* B **13** 1155
[124] Livshits A I and Shluger A L 1999 *Appl. Surf. Sci.* **141** 274
[125] Martin Y, Williams C C and Wickramasighe H K 1987 *J. Appl. Phys.* **61** 4723
[126] Albrecht T R, Gruetter P, Horne D and Rugar D 1991 *J. Appl. Phys.* **69** 668
[127] Uchihashi T, Sugawara Y, Tsukamoto T, Ohta M, Morita S and Suzuki M 1997 *Phys. Rev.* B **56** 9834
[128] Smith J R, Bozzolo G, Banerjea A and Ferrante J 1989 *Phys. Rev. Lett.* **63** 1269
[129] Pethica J B and Sutton A P 1988 *J. Vac. Sci. Technol.* A **6** 2490
[130] Durig U 1995 *Forces in Scanning Probe Methods (NATO ASI Series E 286)* ed H-J Güntherodt, D Anselmetti and E Meyer (Dordrecht: Kluwer) p 191
[131] Good B S and Banerjea A 1996 *J. Phys.: Condens. Matter* **8** 1325
[132] Landman U, Luedtke W D and Ringer E M 1992 *Wear* **153** 3
[133] Muller T, Lohrmann M, Kasser T, Marti O, Mlynek J and Krausch G 1997 *Phys. Rev. Lett.* **79** 5066
[134] Jarvis S P, Yamada H, Yamamoto S-I, Tokumoto H and Pethica J B 1996 *Nature* **384** 247